

# Axial and Radial Diffusivity Measures Detect Brain Tissue Injury in Heart Failure Patients

R. Kumar<sup>1</sup>, M. A. Woo<sup>2</sup>, P. M. Macey<sup>2,3</sup>, G. C. Fonarow<sup>4</sup>, M. A. Hamilton<sup>4</sup>, and R. M. Harper<sup>1,3</sup>

<sup>1</sup>Neurobiology, David Geffen School of Medicine at UCLA, Los Angeles, CA, United States, <sup>2</sup>School of Nursing, UCLA, Los Angeles, CA, United States, <sup>3</sup>Brain Research Institute, UCLA, Los Angeles, CA, United States, <sup>4</sup>Cardiology, UCLA, Los Angeles, CA, United States

## Introduction:

Heart failure (HF) patients show brain tissue loss or injury in autonomic, cognitive, and emotional regulatory areas (1, 2); the regions with tissue injury overlap sites of altered functional MRI signals to autonomic challenges (3, 4). Some structural injury appears on T2-relaxometry procedures, and could result from different pathological processes, including hypoxia/ischemia accompanying perfusion or breathing characteristics in the syndrome. These processes could introduce axonal loss or myelin loss, either independently or in combination; however, T2-relaxometry indicates only generalized tissue damage. In contrast, diffusion tensor imaging-based indices, including axial diffusivity, which measures diffusion of water molecules parallel to the tissue fibers and indicates axonal status, and radial diffusivity, which assesses water diffusion perpendicular to the fibers and primarily shows myelin changes (5) can offer additional insights into types of pathology in HF. We aimed to assess axial and radial diffusivity in HF patients to reveal types of axonal tissue injury present in affected brain sites.

## Materials and methods:

We studied 16 hemodynamically-optimized HF (age, 55.1±7.8 years; 12 male; left ventricular ejection fraction, 28.0±7.0) and 26 control (49.7±10.8 years; 17 male) subjects. Heart failure patients were diagnosed based on national HF diagnostic criteria (6), showed dilated cardiomyopathy and systolic dysfunction, and were classified as New York Heart Association Functional Class II. All HF patients were without prior stroke or carotid vascular disease, recruited from the university hospital and neighboring community, and treated with angiotension-converting enzyme inhibitors or angiotensin receptor blockers, diuretics, and beta blockers. Control subjects were healthy, without history of cardiovascular, cerebrovascular, respiratory, or neurological disorder, with no cardiac or psychotropic medications, and recruited through the university campus. The study protocol was approved by the institutional review board, and all subjects gave written consent before the study. Brain scans of HF and control subjects were collected using a 3.0-Tesla MRI scanner (Magnetom Tim-Trio; Siemens) with an 8-channel phased-array head coil. Diffusion tensor imaging was performed using a single-shot echo-planar imaging with twice-refocused spin-echo pulse sequence (TR = 10,000 ms; TE = 87 ms; FA = 90°; BW = 1346 Hz/ pixel; matrix size = 128×128; FOV = 230×230 mm; thickness = 2.0 mm, no interslice-gap, b = 0 and 700 s/mm<sup>2</sup>, diffusion gradient directions = 12). We used the parallel imaging technique, generalized autocalibrating partially parallel acquisition, with an acceleration factor of two, and four DTI series were acquired separately, with the same imaging protocol for subsequent averaging. We processed data using the SPM5, DTI-Studio, and Matlab-based custom software. Using diffusion and non-diffusion-weighted images, diffusion tensors were calculated and principal eigenvalues ( $\lambda_1$ ,  $\lambda_2$ , and  $\lambda_3$ ) were derived by diagonalizing the diffusion tensor matrix. Using principal eigenvalues, axial diffusivity ( $\lambda_{\parallel} = \lambda_1$ ), and radial diffusivity [ $\lambda_{\perp} = (\lambda_2 + \lambda_3)/2$ ] maps were derived from each DTI series. Axial and radial diffusivity maps and b0 images were realigned and averaged. Axial and radial diffusivity maps and b0 images were normalized to Montreal Neurological Institute space, and normalized maps were smoothed. The normalized and smoothed axial and radial diffusivity maps were compared voxel-by-voxel between groups using analysis of covariance (covariates, age and gender; uncorrected, p<0.001). Statistical parametric maps, showing significant differences in axial and radial diffusivity between groups, were created for sites showing increased radial diffusivity only, increased axial diffusivity only, and both increased axial and radial diffusivity, and overlaid onto mean b0 image, derived from normalized images of all HF and control subjects, for structural identification.

## Results:

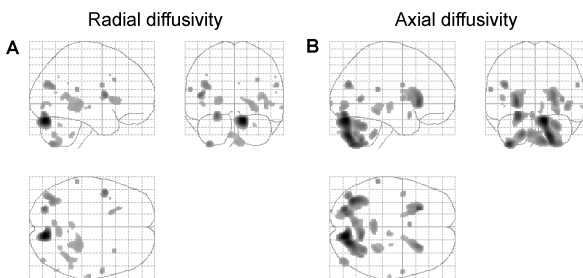


Fig.1: Brain areas showing increased axial and radial diffusivity in HF compared to control subjects.

No significant differences in age, gender, or body mass index emerged between the groups. Multiple brain regions in HF showed significantly increased radial (Fig. 1A) and axial (Fig. 1B) diffusivity measures over control subjects. No brain regions showed increased axial or radial diffusivity in control subjects over HF.

Significantly increased radial, with no significant change in axial diffusivity appeared in right temporal and frontal white matter. Increased axial, with no significant change in radial diffusivity emerged in the right internal capsule, bilateral anterior insula and caudate, mid thalamus, and bilateral superior and right inferior cerebellar peduncles, extending to cerebellar cortex. Multiple brain regions showed both higher axial and radial diffusivity, including parietal and left occipital cortex, left internal capsule, and right posterior thalamus extending to hippocampus, bilateral cerebellar cortex, and dorsal medulla.

## Discussion:

Axial and radial diffusivity measures showed significant axonal and myelin injury, with reduced axonal density or caliber appearing in internal capsule and cerebellar regions, and axonal damage with reduced myelin emerging in temporal and frontal areas. Other brain areas, including internal capsule and dorsal medial medulla largely showed both myelin and axonal injury. More-extensive tissue injury appeared in the cerebellum and insular cortices, areas that have significant autonomic outflow regulatory and coordination roles, respectively, and could contribute significantly to the impaired cardiovascular characteristics found in HF. The findings indicate central nervous system injury accompanies the HF condition, perhaps resulting from a combination of ischemic or hypoxic processes associated with the syndrome, and can further exacerbate its characteristics.

## References:

1. Woo, M.A., Kumar, R., Macey, P.M., Fonarow, G.C., Harper, R.M. *J. Card. Fail.* 15: 214-223, 2009.
2. Woo, M.A., Macey, P.M., Fonarow, G.C., Hamilton, M.A., Harper, R.M. *J. Appl. Physiol.* 95: 677-84, 2003.
3. Woo, M.A., Macey, P.M., Keens, P.T., Kumar, R., Fonarow, G.C., Hamilton, M.A., Harper, R.M. *Congest. Heart Fail.* 13: 29-35, 2007.
4. Woo, M.A., Macey, P.M., Keens, P.T., Kumar, R., Fonarow, G.C., Hamilton, M.A., Harper, R.M. *J. Card. Fail.* 11: 437-446, 2005.
5. Song, S.K., Sun, S.W., Ramsbottom, M.J., Chang, C., Russell, J., Cross, A.H. *Neuroimage* 17: 1429-1436, 2002.
6. Radford, M.J., Arnold, J.M., Bennett, S.J., Cinquegrani, M.P., Cleland, J.G., Havranek, E.P., et al. *Circulation* 112: 1888-1916, 2005.

**Grants:** Supported by NR-009116.